A Facile Dye-Initiated Polymerisation of Lactide-Glycolide Generates Highly Fluorescent PLGA for Enhanced Characterisation of Cellular Delivery.

Mohammad A Al-natour,[1,2,3†] Mohamed D Yousif,[1†] Robert Cavanagh,[1] Amjad Selo,[1] Edward A Apebende,[4] Amir Ghaemmaghami,[2] Dong-Hyun Kim,[1] Jonathan W Aylott,[1] Vincenzo Taresco,[1,4*] Veeren M Chauhan,[1*] and Cameron Alexander.[1*]

[1] School of Pharmacy, Boots Science Building, University of Nottingham, Nottingham, NG7 2RD, UK

[2] Division of Immunology, School of Life Sciences, Faculty of Medicine and Health Sciences, Queen's Medical Centre, University of Nottingham, Nottingham, United Kingdom

[3] The Faculty of Pharmacy and Medical Sciences, University of Petra, Amman, Jordan.

[4] School of Chemistry, University of Nottingham, Nottingham, NG7 2RD, UK

Poly (lactic-co-glycolic acid), fluorescent, ring opening polymerisation, intracellular delivery, intestinal delivery, THP-1 macrophages,

Poly (lactic-co-glycolic acid) (PLGA) is a versatile synthetic co-polymer that is widely used in pharmaceutical applications. This is because it is well-tolerated in the body and co-polymers of varying physicochemical properties are readily available *via* ring-opening polymerisation. However, native PLGA polymers are hard to track as drug delivery carriers when delivered to sub-cellular spaces due to the absence of an easily accessible 'handle' for fluorescent labelling. Here we show a one-step, scalable, solvent-free, synthetic route to fluorescent blue (2-aminoanthracene), green (5-aminofluorescein) and red (Rhodamine-6G) PLGA, in which every polymer chain in the sample is fluorescently labelled. The utility of initiator-labelled PLGA was demonstrated through the preparation of nanoparticles, capable of therapeutic sub-cellular delivery to T-helper-precursor-1 (THP-1) macrophages, a model cell line for determining *in vitro* biocompatibility and particle uptake. Super resolution confocal fluorescence microscopy imaging showed that dye initiated PLGA nanoparticles were internalised to punctate regions and retained bright fluorescence over at least 24 hrs. In comparison, PLGA nanoparticles with 5-aminofluorescein introduced by conventional nano-precipitation/encapsulation, showed diffuse and much lower fluorescence intensity in the same cells and over the same time periods. The utility of this approach for *in vitro* drug delivery experiments was demonstrated through the concurrent imaging of the fluorescent drug doxorubicin (λ_{ex} 480 nm, λ_{em} 590 nm) with carrier 5-aminofluorescein PLGA, also in THP-1 cells, in which the intracellular locations of the drug and the polymer could be clearly visualised. Finally, the dye-labelled particles were evaluated in an *in vivo* model, via delivery to the nematode *C. elegans*, with bright fluorescence again apparent in the internal tract after 3 hrs. The results presented in this manuscript highlight the ease of synthesis of highly fluorescent PLGA, which could be used to augment tracking of future therapeutics and accelerate *in vitro* and *in vivo* characterisation of delivery systems prior to clinical translation.

Poly (lactic-co-glycolic acid) (PLGA) is a synthetic biocompatible copolymer widely used for biomedical applications.[1-4] PLGA particulate carriers have been used to deliver therapeutics ranging from low molecular weight drugs, peptides and proteins, through to nucleic acids, vaccines and cells.[1, 5-10] In addition, PLGA-based scaffolds based on colloidal particles, hydrogels and fibres have been extensively explored for regenerative medicine.[11-13]

For therapeutic applications, it is essential to monitor the kinetics of tissue and cellular drug uptake, specific organ accumulation after systemic administration, *in vivo* bio-distribution and intracellular fate of these therapeutics.[14] For *in vitro* studies, the most common strategy used is to load PLGA nanoparticles with fluorophores, which can then be imaged with wide field or confocal fluorescence microscopy to determine polymer biodistri-

bution.[15] However, the major drawback associated with this approach has been the separation and leakage of the fluorophore from the PLGA nanoparticles, which can result in measurement and experimental artefacts. This is because it is extremely challenging to distinguish between the signal from the loaded nanoparticles and unbound leaking fluorophores,[16] which can lead to an overestimation of the nanoparticle uptake.[1] Furthermore, free fluorophores may interact with biological systems and can induce unwanted biochemical processes, while burst release of dyes from nanoparticles can result in transient high local concentrations and potential; toxicity.[17] To enhance fluorescence imaging of PLGA nanoparticle biodistribution and to overcome the challenges associated with fluorophore leaching, PLGA can be covalently linked to fluorophores.[18] However, PLGA itself has a limited number of easily modifiable functional groups, i.e. the hydroxyl and carboxyl termini, which restricts the efficacy of fluorophore labelling. In a typical example, a labelling efficiency of 65% was achieved when 5-aminofluorescein was reacted with PLGA.[19] Other routes to functionalized PLGA have required multiple steps and were performed in organic solvents, which in turn renders scale-up challenging.[20]

Our motivation was to overcome fluorophore leakage and the low efficiency of PLGA labelling through a simple, solvent free, one-step reaction to prepare fluorescent polymers with a label on each chain. This was achieved using fluorophores with active nucleophilic moieties as initiators in a solvent-free ring opening polymerisation (ROP) reaction of lactide (LA) and glycolide (GA) monomers.

We used this method to synthesise three different fluorescently labelled PLGA copolymers, by ring-opening LA and GA in the presence of 2-aminoanthracene (2AA, blue), 5-aminofluorescein (5AF, green) and Rhodamine-6G (R6G, red). The newly synthesised polymers were then used to fabricate nanoparticles *via* a solvent displacement method.

The initial one-step synthesis used a conventional ($Sn(Oct)_2$) catalysed ring opening polymerization route[21] and fluorophores (2AA, 5AF and R6G) with pendant amines were used as the nucleophiles. The mechanism of this reaction occurs through anionic ROP, in which the initial dye amine attacks a carbonyl group in the LA or GA ring.

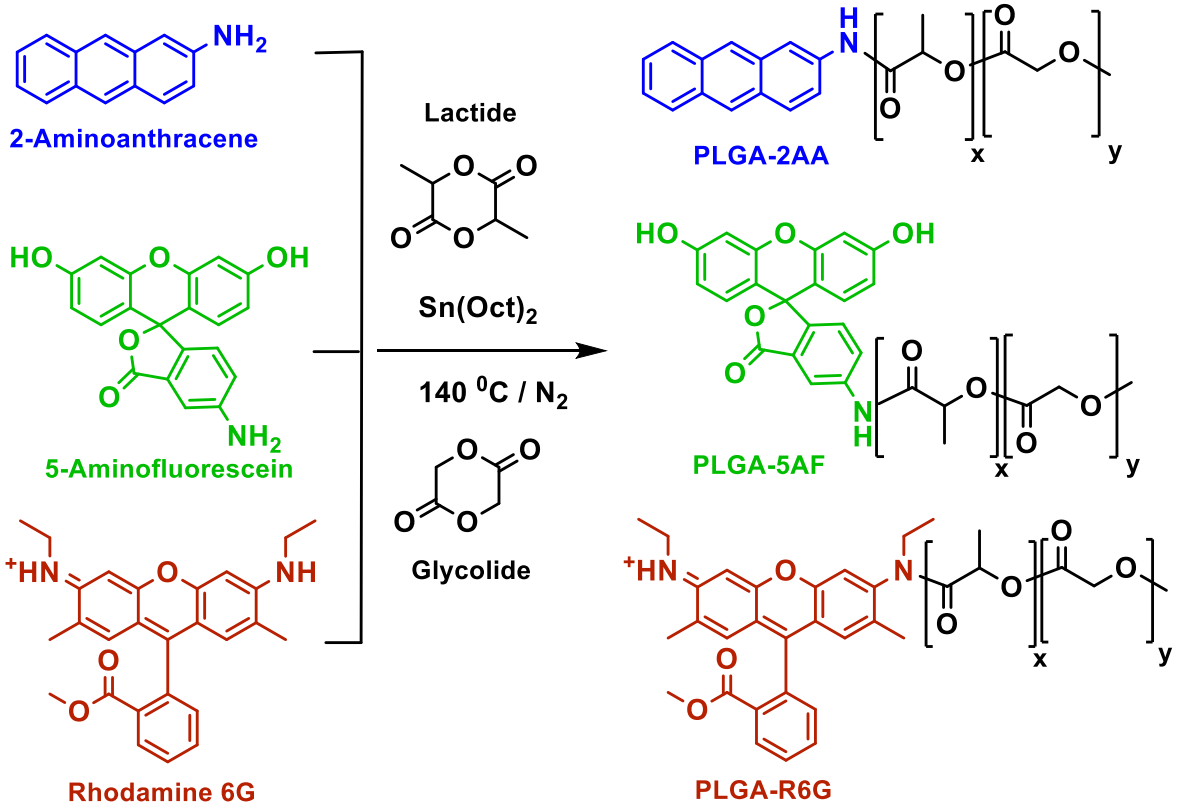

Figure 1. Schematic representation of PLGA-2AA, PLGA-5AF, PLGA-R6G and synthesis using ROP. All reactions were conducted at 140 °C under Nitrogen (N_2), catalysed by tin (II) 2-ethylhexanoate (Sn $(Oct)_2$).

This frees a nucleophilic hydroxyl group which opens further LA and GA rings, such that the reaction continues until all the LA and GA are consumed. The resulting polymers were denoted as PLGA-AA, PLGA-5AF and PLGA-R6G (Figure 1B) and their structures were confirmed using H^1 NMR spectroscopy (Figures S1, S2 and S3, respectively). The kinetics of the reaction (for %AFPLGA, as a model material) was followed and analysed (Figure S4). These experiments showed that high conversion to polymer was reached after 60 mins of reaction (Figure S4A and B). By leaving the reaction for an additional 2 hours, the conversion reached a plateau value and the linearity was lost (Figure S4C). In the case of 2AA initiated ROP reaction a concurrent loss in molar mass control and also a drop in final yield in polymer were observed. In fact, when 2AA was adopted as initiator after 60 mins a Đ of 1.3 was registered (Table 1) while a Đ of 1.8 was reached after 180 mins. On the other hand, a constant value of 1.2 was observed for 5AF-initiated PLGA independently from the reaction time. This may imply an increasing instability with time, under reaction

conditions, and triggering side reactions (unzipping or branching) in the presence of 2AA. All the synthesised polymers showed a narrower molecular weight distribution compared to the commercially-available labelled-PLGA (Đ ~ 1.55 Figure S5). Moreover, the presence of the dye linked to the polymeric chain was confirmed by GPC measurements carried out with UV-vis-RI tandem detectors. The two traces overlapped for all the synthesised polymers confirming the presence of the dye on the polymer chain (Figure S5 and insets).

The yields of purified polymers for PLGA-AA, PLGA-5AF and PLGA-R6G, were 65% (grey solid), 65% (deep orange solid) and 60% (light pink solid), respectively (Table 1). Following synthesis, PLGA nanoparticles were produced via a controlled flow solvent/anti-solvent nanoprecipitation methodology. Both fluorescent and unlabelled PLGA NPs had comparable hydrodynamic diameters, centred at 100 nm, and with zeta potentials of approximately -40 mV (Table S1). TEM imaging confirmed that the fluorescent nanoparticles were of low size dispersity, and that there were no obvious differences between the polymers used to manufacture the nanoparticles (Figure S6), which is in accord with previously reported literature.[22] To compare the relative emission intensities of newly prepared fluorescent-dye-initiated PLGA nanoparticles versus unlabelled PLGA nanoparticles loaded with the analogous dye (5-AF), fluorescence spectroscopy was conducted. PLGA-5AF nanoparticles were found to be ~ 12.5x brighter than PLGA nanoparticles loaded with 5-AF ($p<0.0001$). Furthermore, 24 hrs after initial preparation, the fluorescence of PLGA-5AF nanoparticles had decreased by ~3 % whereas for PLGA nanoparticles loaded with 5-AF, the fluorescence intensity reduced by 45% (Figure S7A). These results indicated PLGA nanoparticles prepared using fluorophore linked PLGA were significantly brighter ($p<0.0001$) and demonstrated enhanced stability after 24 hours of storage, thus suggesting their promise for medium and long-term experimentation. In addition, 100 nm nanoparticles prepared from PLGA polymerised from 5-aminofluorescein were ~8-fold brighter than a commercially available fluorescent-labelled PLGA formulated into analogous 100 nm particles (Figure S8). It is also important to note AF, a fluorescein, is a pH sensitive fluorophore. As such the fluorescence intensity of fluorescein derivatives is quenched in acidic environments,[17, 23] such as those found in endosomal/lysosomal compartments.[24] Therefore, observation of live cell behaviour with PLGA-AF polymeric nanoparticles, in the absence of a ratiometric control can be challenging. This effect can be overcome through chemical fixation and resuspension of cells for analysis in buffered media, such as phosphate buffered saline (pH 7.4), to equilibrate cellular pH where AF fluorescence intensity is not diminished (please see ESI).

The effects of these PLGA nanoparticles on cell metabolism were then evaluated through AlamarBlue assays and the intracellular location of internalized particles further investigated with wide field fluorescence microscopy in human T-helper-precursor-1 (THP-1) macrophages, a model cell line for determining *in vitro* biocompatibility and particle uptake.[25] These assays directly compared PLGA NPs (PLGA-AA, PLGA-AF and PLGA-R6G), with commercially produced unlabelled PLGA (PLGA), fluorophore loaded PLGA (AF loaded NPs) and a commercially available green fluorescent PLGA. Cells were challenged with increasing nanoparticle concentrations (50-500 µg/mL) for 24 hrs.

Table 1. Labelled PLGA (Blue, green and red) synthesis, composition (monomer ratio), molecular weight ($g.mol^{-1}$) and yield. NMR calculated molar mass (M Cal), and determined molar masses (M_n, M_w via GPC, using PMMA standards as calibrants) and poly dispersity Index (Đ). LA = lactide, GA = glycolide.

Polymer	Feed ratio (mol %)			Product ratio (mol %)			Molecular weight ($g\ mol^{-1}$)			Đ	Yield (%)
	LA	GA	Dye	LA	GA	Dye	M (calc)	M_n	M_w		
PLGA-2AA	59	39	2	46	32	2	15000	5500	7260	1.3	65%
PLGA-5AF	59	39	2	47	40	2	11600	8700	10440	1.2	65%
PLGA-R6G	59	39	2	53	33	2	11900	5600	7840	1.4	60%

Fluorescently labelled PLGA NPs were well-tolerated by the cells, as more than 75% of cells were shown to be actively metabolising at 500 µg/mL (Figure S7B). More importantly, no significant difference was observed in cell viability between PLGA-AA, PLGA-AF, PLGA-R6G, PLGA (commercial), AF loaded PLGA NPs and TEM imaging confirmed that the fluorescent nanoparticles were of low size dispersity, and that there were no obvious differences between the polymers used to manufacture the nanoparticles (Figure S6), which is in accord with previously reported literature.[22] To compare the relative emission intensities of newly prepared fluorescent-dye-initiated PLGA nanoparticles versus unlabelled PLGA nanoparticles loaded with the analogous dye (5-AF), fluorescence spectroscopy was conducted. PLGA-5AF nanoparticles were found to be ~ 12.5x brighter than PLGA nanoparticles loaded with 5-AF ($p<0.0001$). Furthermore, 24 hrs after initial preparation, the fluorescence of PLGA-5AF nanoparticles had decreased by ~3 % whereas for PLGA nanoparticles loaded with 5-AF, the fluorescence intensity reduced by 45% (Figure S7A). These results indicated PLGA nanoparticles prepared using fluorophore linked PLGA were significantly brighter ($p<0.0001$) and demonstrated enhanced stability after 24 hours of storage, thus suggesting their promise for medium and long-term experimentation.

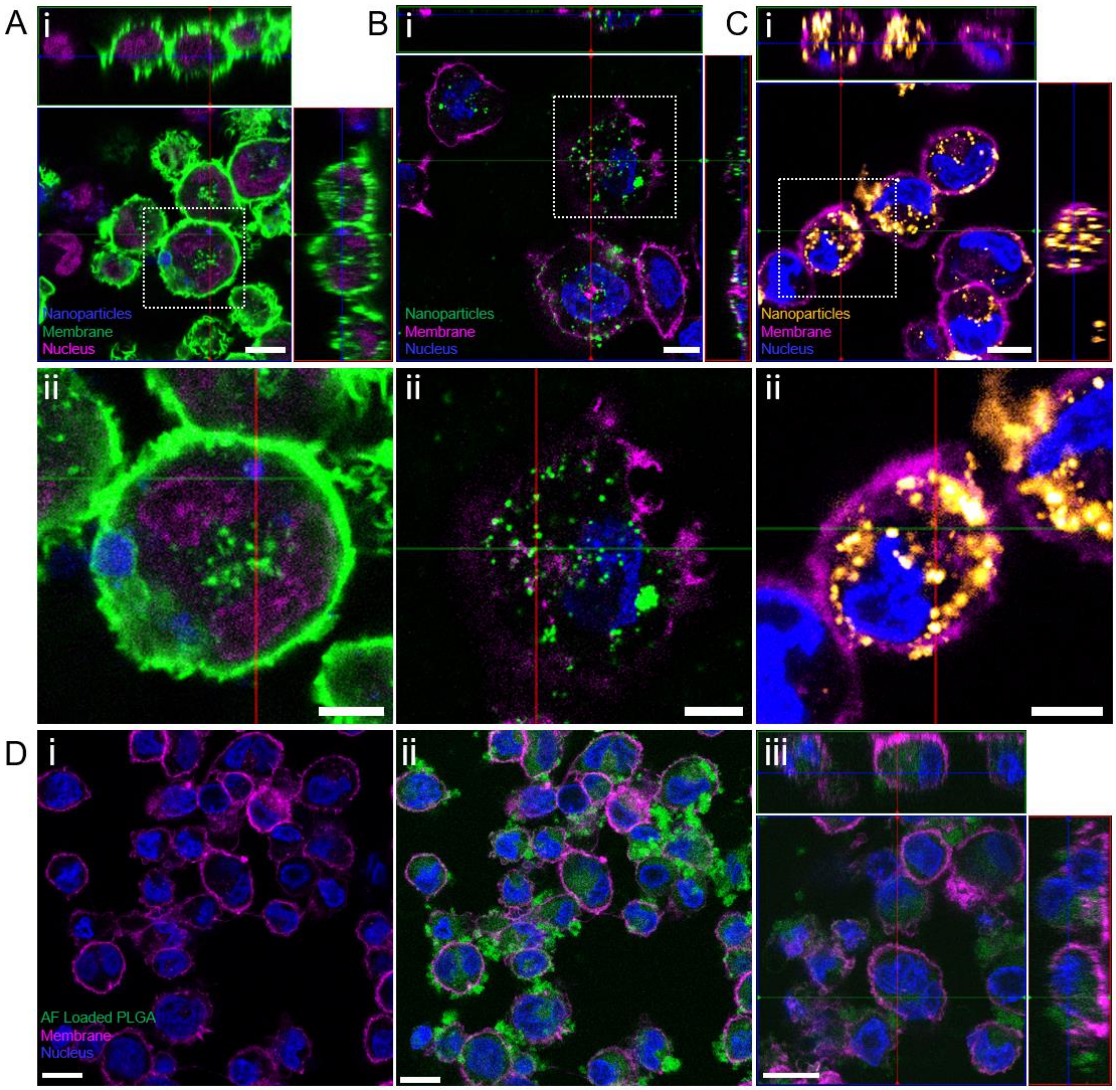

Figure 2. Super-resolution microscopy images of fluorescent (A) blue, (B) green and (C) red PLGA nanoparticles (100 µg/mL, 3 hrs) in activated THP-1 macrophages. Cells were fixed and stained for cytoskeleton (A) Alexafluor 488, green and (B&C) Alexafluor 647, magenta) and nucleus (A) Draq 5 nucleus, magenta and (B&C) Hoechst nucleus, blue). Images Aii, Bii and Cii are zoomed regions of interest, highlighted in Ai, Bi and Ci, respectively. Scale bar for Ai, Bi & Ci = 20 µm and Aii, Bii & Cii = 10 µm. (D) Fluorescence images of PLGA loaded with 5AF (100 µg/mL)) treated THP-1 cells. Cells were fixed and stained for cytoskeleton (Alexafluor 647, magenta) and nucleus (Hoechst, blue). Image (Di) and (Dii) show the same region of interest, however, (Di) was acquired under the same experimental laser power as (Bi), whereas Figure (Dii) was acquired at 8 times the laser power required to excite green fluorescence. (Dii) Orthogonal cross section of THP-1 cells showing internalisation of 5AF fluorophore. Scale bar = 20 µm.

The effects of these PLGA nanoparticles on cell metabolism were then evaluated through AlamarBlue assays and the intracellular location of internalized particles further investigated with wide field fluorescence microscopy in human T-helper-precursor-1 (THP-1) macrophages, a model cell line for determining *in vitro* biocompatibility and particle uptake.[25] These assays directly compared PLGA NPs (PLGA-AA, PLGA-AF and PLGA-R6G), with commercially produced unlabelled PLGA (PLGA), fluorophore loaded PLGA (AF loaded NPs) and a commercially available green fluorescent PLGA. Cells were challenged with increasing nanoparticle concentrations (50-500 µg/mL) for 24 hrs. Fluorescently labelled PLGA NPs were well-tolerated by the cells, as more than 75% of cells were shown to be actively metabolising at 500 µg/mL (Figure S7B). More importantly, no significant difference was observed in cell viability between PLGA-AA, PLGA-AF, PLGA-R6G, PLGA (commercial), AF loaded PLGA NPs and commercially available dye-conjugated nanoparticles at all experimental concentrations ($p<0.01$). Therefore, a concentration of 100 µg/mL was used for subsequent experiments.

To investigate the subcellular localisation of fluorescently labelled PLGA NPs (100 µg/mL), THP-1 cells were dosed with particles for 3 hours and imaged using super-resolution confocal microscopy. All fluorescent PLGA NPs were internalised as demonstrated by the orthogonal cross-sections (Figure 2 Ai-Ci). As apparent from Figure 2A-D, dye-initiated PLGA nanoparticles (PLGA-AF) demonstrated rather different fluorescence responses, when compared to fluorophore loaded PLGA nanoparticles. Images A, B and C show the dye-initiated nanoparticles localized in bright fluorescent regions, whereas Figure 2Di indicated that the dye-loaded particles were less bright and more diffuse in the cells. For Figures 2Di and 2Dii the same regions of interest are shown; however, Figure 2Di was acquired under the

same experimental laser power as Figure 2Bi, whereas Figure 2Dii was acquired at 8 times the laser power in order to excite the same level of fluorescence as occurred from the dye-initiated nanoparticles in Bii.

In addition, the images shown in Figures Aii, Bii and Cii indicated that the dye-initiated nanoparticles were present in discrete sub-cellular vesicles. This suggested that the dyes were retained with the polymers in nanoparticles which were stable to endocytic pathways and intracellular transport processes. In contrast, close analysis of Figures 2Dii and 2Diii revealed no clear punctate regions, implying that the PLGA NPs loaded with AF released their contents into a diffuse intracellular space and that dye and nanoparticles were most probably no longer co-localised. These data were further corroborated with analysis of the dye-initiated PLGA nanoparticles in comparison with the commercial dye-conjugated 100 nm PLGA nanoparticle formulation. As apparent in Figure S9, both nanoparticle formulations were localised in punctate regions in the THP-1 cells, again indicating that covalent attachment of dyes to the polymer chains prevented general cytosolic fluorescence due to generalised dye diffusion. The dye-initiated PLGA nanoparticles were also notably brighter than the commercial samples (Figure S9, as evidenced by comparison of the images optimised for brightness for each nanoparticle type.

In order to demonstrate the advantages of the single chain fluorescently labelled PLGA (PLGA-AF) for tracing the intracellular fate of nanomaterials in a representative drug delivery experiment, the polymers were formed into nanoparticles containing encapsulated doxorubicin hydrochloride. This DNA intercalating anticancer drug exhibits red fluorescence (λ_{ex} 480 nm, λ_{em} 590 nm) and has been very widely used both in laboratory studies and in the clinic.[26-29] We selected THP-1 cells for these experiments because they are non-proliferative, which makes them tolerant to doxorubicin and therefore a good model to study its cellular delivery. Accordingly, doxorubicin loaded PLGA-AF NPs were fabricated and dosed to activated THP-1 cells at sub toxic concentrations (100 µg/ml, 3 hours).

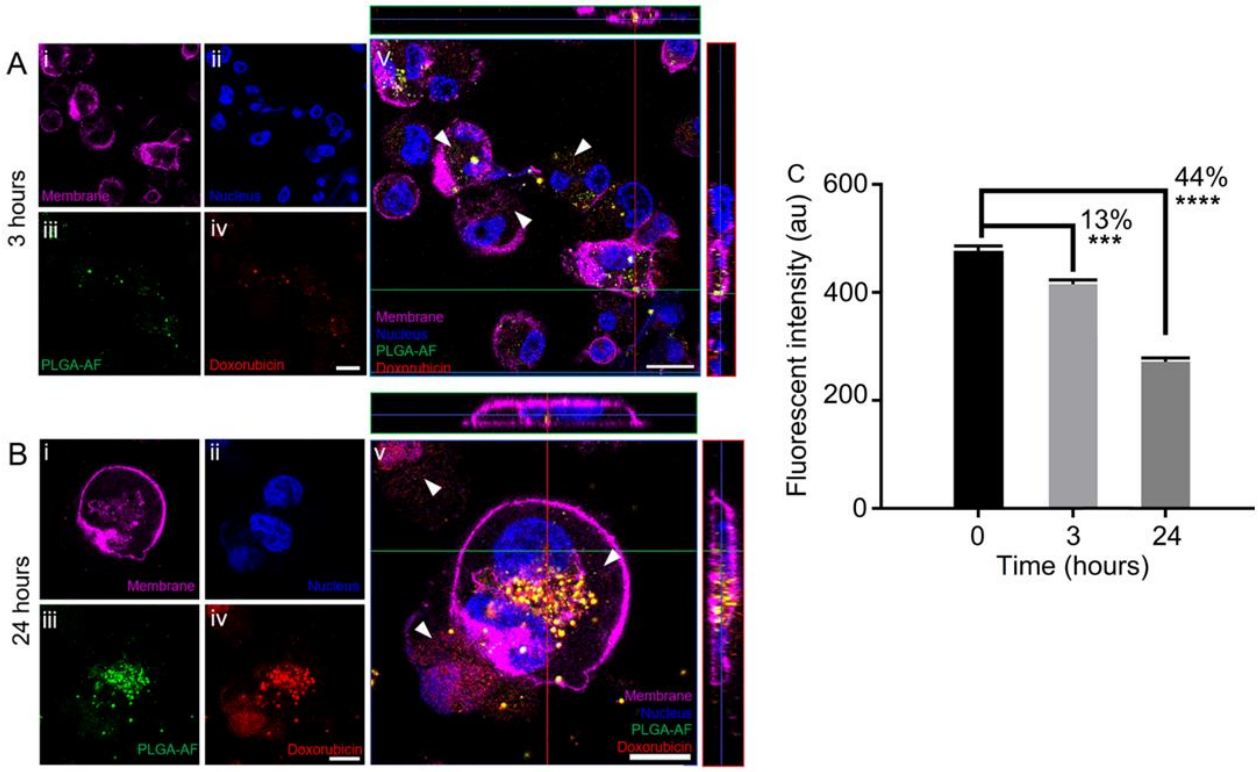

Figure 3. The uptake of doxorubicin loaded PLGA NPs by activated THP-1 cells. Cells were treated with RPMI complete medium containing (100 µg/mL) of doxorubicin loaded NPs for 3 hours and imaged after (A) 3 hours and (B) 24 hours. Following exposure cells were fixed and stained for the cytoskeleton (magenta) and nucleus (blue). Arrowheads in A (v) and B (v) show distribution of doxorubicin in the cells after 3 and 24 hours, respectively. (C) Comparison of fluorescence intensity of doxorubicin in PLGA-5AF loaded nanoparticles after 0, 3 and 24 hours. (A&B) Scale bar = 20 µm and (C) error bars represent standard deviation (n=3).

Figure 3 shows that doxorubicin fluorescence (red) was distributed in regions of interest away from PLGA-AF (green) when imaged after 3 hours (Figure 3A) and after 24 hours (Figure 3B). Through further analysis of microscopy images, the data suggests doxorubicin/PLGA-AF formulated nanoparticles (yellow), appear to reside in punctate vesicles, which were likely to be lysosomal or endosomal compartments. Doxorubicin was found to diffuse away from these regions and the labelled polymers, while the aminofluorescein dye remained attached to the polymers over these time periods. However, the extent of any degradation of the PLGA chains during the cell assays could not be ascertained other than that no fragments were able to diffuse away at the same rate as the small molecule drug.

The release of doxorubicin from PLGA-AF nanoparticles was confirmed in parallel release assays in aqueous media: after 24 hours the fluorescence intensity of PLGA nanoparticles loaded with doxorubicin by nanoprecipitation had dropped by 44 % (Figure 3C). These results highlighted the advantages of dye-initiated

PLGA during the monitoring of therapeutic delivery to show the subcellular distribution of both drug and carriers *in vitro*.

The culminating experiments aimed to demonstrate the advantages of the single-chain labelled PLGA *in vivo*. The nematode *C. elegans* was chosen as an accessible model to study *in vivo* biodistribution of the labelled nanoparticles (Figure 4). Synchronized cycles of *C. elegans* (L4-young adult stages) were washed with sterile deionised water prior to dosing, and ~300 nematodes were the exposed to a range of PLGA nanoparticles at 100 µg/mL (n = 3) for 3 hours. The nematodes were washed again before examination and collected for fluorescence microscopy imaging.

The images in Figure 4 clearly show the internalization of the nanoparticles and their localization in the digestive tracts of the nematodes. The key result in these experiments was the different localisation of fluorescence arising from the dyes encapsulated in the nanoparticles and the fluorescence from the dyes covalently-linked to the PLGA chains. The encapsulated rhodamine B dye diffused throughout the then nematode digestive tract within 12 hours (Figure 4B) and was not fully co-localised with the fluorescein signals from the nanoparticles (Figure 4D, E). For the dye-initiated NPs, bright fluorescence was apparent in discrete regions of the nematodes (Figure 4 G-H) and this was retained throughout the experiment without any obvious changes in the behaviour or viability of the worms (Figure S11). These experiments indicated good tolerability of the nanoparticles in addition to the retention of their bright fluorescence *in vivo*. In addition, and of crucial importance, the data indicated the advantage of using covalently-linked dyes, in which every polymer chain was tagged, to track *in vivo* transport of nanoparticles in the presence of encapsulated labels and/or actives.

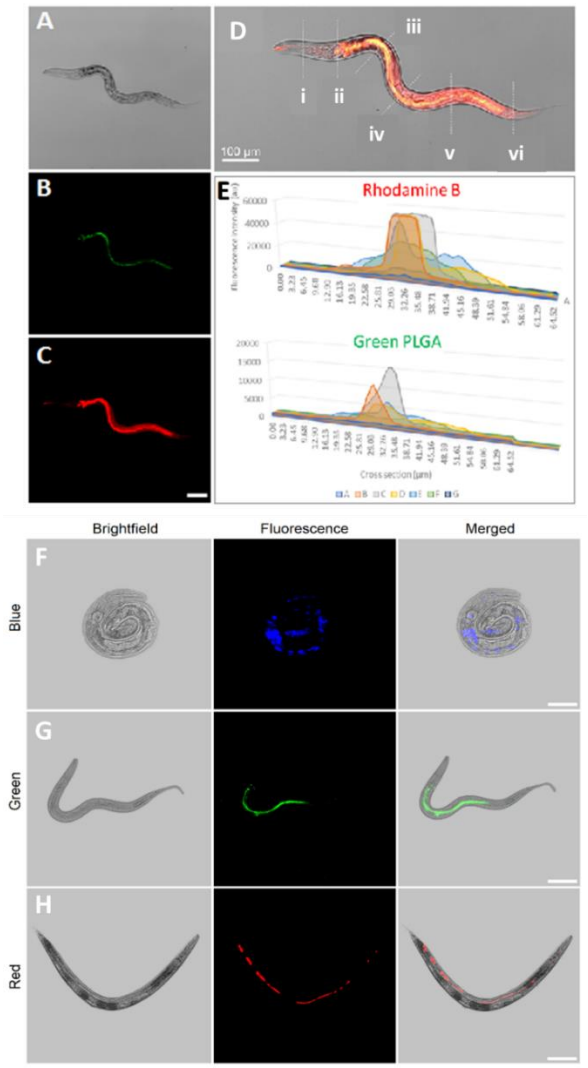

Figure 4. Fluorescence microscopy images of representative *C. elegans* nematodes following incubation with PLGA-based nanoparticles. Panels (A-E) show nematodes exposed over 12 hrs to PLGA-5AF NPs with encapsulated Rhodamine-B, with images (A) brightfield, (B) green (5-AF channel), (C) red (rhodamine channel) and (D) merged. Panel (D) is segmented (i-vi) to show the regional distribution of Rhodamine-B, and (E) shows the fluorescence intensities of Rhodamine-B and 5-AF in the various anatomical parts/sections of the nematode. The different distributions of 5-AF, arising from the PLGA chains in the nanoparticles and the free rhodamine indicate the utility of the labelled polymers to track in vivo transport in the presence of released actives. In panels (F-H), fluorescence images of *C. elegans* challenged with the various blue, green and red fluorescent PLGA nanoparticles are shown. Scale bar blue = 100µm, green = 200 µm red = 200 µm.

CONCLUSIONS

This study described the synthesis of fully fluorescently labelled PLGA using three different fluorophores via a single step ROP reaction under solvent-free conditions. The resultant dye-initiated PLGA polymers were able to self-assemble into well-defined nanoparticles which were significantly more bright in fluorescence microscopy when compared to dye-encapsulated and commercially available dye-linked analogues. The nanoparticles were readily internalised by activated THP-1 macrophages and exhibited a comparable cytocompatibility profile to commer-

cially available PLGA *in vitro*. In addition, the stability of the fluorescent dye-polymer link was demonstrated by retention of the label in punctate regions of the THP1 cells, again in contrast to dye-encapsulated PLGA, which released the entrapped label over time. In turn this property was exploited in a model drug delivery experiment in which the separate intracellular locations of a released drug, doxorubicin, and the carrier polymers were shown in THP-1 cells. The preliminary *in vivo* study in *C. elegans* further exemplified the use of these bright and stable nanoparticles, with clear differences between the distribution of released dye and dye-initiated PLGA nanoparticles. We believe this synthetic strategy may be further used to prepare a range of intrinsically labelled biodegradable polymers which could greatly facilitate the tracking of delivery systems in sub-cellular locations in the presence of multiple therapeutic constructs. In turn, these materials will allow better characterization of delivery pathways and cellular transport kinetics to accelerate clinical translation.

ASSOCIATED CONTENT

Full experimental methods are provided in the Supporting Information including NMR spectra of polymers, GPC chromatograms, TEM, DLS and zeta potential data, and details of cell and nematode culture. This material is available free of charge via the Internet at http://pubs.acs.org.

AUTHOR INFORMATION

Corresponding Authors *

* Veeren M Chauhan, Vincenzo Taresco, Cameron Alexander, School of Pharmacy, University of Nottingham, Nottingham NG7 2RD, UK.
E-mail: Veeren.Chauhan@nottingham.ac.uk, Vincenzo.Taresco@nottingham.ac.uk, Cameron.Alexander@nottingham.ac.uk.

Author Contributions

†Authors MAAN & MDY contributed equally. The manuscript was written through contributions of all the authors. All authors have given approval to the final version.

Funding Sources

This work was supported by the Engineering and Physical Sciences Research Council [grant numbers EP/P006485/1, EP/N03371X/1, EP/H005625/1]. Super-resolution microscopy was conducted in the School of Life Sciences Imaging facility (SLIM), which is supported by the Biotechnology and Biological Sciences Research Council [Grant number BB/L013827/1]. This work was also funded by the Royal Society [Wolfson Research Merit Award WM150086 (to CA)]. Financial and in-kind support from a consortium of industrial users is also acknowledged (VMC & JWA).

Data access statement

All raw data created during this research are openly available from the corresponding author cameron.alexander@nottingham.ac.uk) and at the University of Nottingham Research Data Management Repository (https://rdmc.nottingham.ac.uk/) and all analysed data supporting this study are provided as supplementary information accompanying this paper.

ACKNOWLEDGMENTS

The authors are extremely grateful to the University of Petra for their financial support (MA). The authors are extremely grateful to Dr Robert Markus for help with the super resolution microscopy and Transmission Electron Microscopy, respectively

REFERENCES

1. Xu, P.; Gullotti, E.; Tong, L.; Highley, C. B.; Errabelli, D. R.; Hasan, T.; Cheng, J.-X.; Kohane, D. S.; Yeo, Y., Intracellular Drug Delivery by Poly(lactic-co-glycolic acid) Nanoparticles, Revisited. Molecular Pharmaceutics 2009, 6 (1), 190-201.

2. Danhier, F.; Ansorena, E.; Silva, J. M.; Coco, R.; Le Breton, A.; Préat, V., PLGA-based nanoparticles: An overview of biomedical applications. Journal of Controlled Release 2012, 161 (2), 505-522.

3. Martins, C.; Sousa, F.; Araujo, F.; Sarmento, B., Functionalizing PLGA and PLGA Derivatives for Drug Delivery and Tissue Regeneration Applications. Advanced Healthcare Materials 2018, 7 (1).

4. Ding, D. W.; Zhu, Q. D., Recent advances of PLGA micro/nanoparticles for the delivery of biomacromolecular therapeutics. Materials Science & Engineering C-Materials for Biological Applications 2018, 92, 1041-1060.

5. Mir, M.; Ahmed, N.; Rehman, A. U., Recent applications of PLGA based nanostructures in drug delivery. Colloids and Surfaces B-Biointerfaces 2017, 159, 217-231.

6. Man, D. K. W.; Casettari, L.; Cesp, M.; Bonacucina, G.; Palmieri, G. F.; Sze, S. C. W.; Leung, G. P. H.; Lam, J. K. W.; Kwok, P. C. L., Oleanolic Acid Loaded PEGylated PLA and PLGA Nanoparticles with Enhanced Cytotoxic Activity against Cancer Cells. Molecular Pharmaceutics 2015, 12 (6), 2112-2125.

7. Fu, J.; Sun, F.; Liu, W.; Liu, Y.; Gedam, M.; Hu, Q.; Fridley, C.; Quigley, H. A.; Hanes, J.; Pitha, I., Subconjunctival Delivery of Dorzolamide-Loaded Poly(ether-anhydride) Microparticles Produces Sustained Lowering of Intraocular Pressure in Rabbits. Mol Pharm 2016, 13 (9), 2987-95.

8. Thomas, C.; Rawat, A.; Hope-Weeks, L.; Ahsan, F., Aerosolized PLA and PLGA Nanoparticles Enhance Humoral, Mucosal and Cytokine Responses to Hepatitis B Vaccine. Molecular Pharmaceutics 2011, 8 (2), 405-415.

9. Cun, D.; Jensen, D. K.; Maltesen, M. J.; Bunker, M.; Whiteside, P.; Scurr, D.; Foged, C.; Nielsen, H. M., High loading efficiency and sustained release of siRNA encapsulated in PLGA nanoparticles: quality by design optimization and characterization. European Journal of Pharmaceutics and Biopharmaceutics 2011, 77 (1), 26-35.

10. Martins, C.; Chauhan, V. M.; Selo, A. A.; Al-Natour, M.; Aylott, J. W.; Sarmento, B., Modelling protein therapeutic co-formulation and co-delivery with PLGA nanoparticles continuously manufactured by microfluidics. Reaction Chemistry & Engineering 2020.

11. Wang, W.; Liang, H.; Cheikh Al Ghanami, R.; Hamilton, L.; Fraylich, M.; Shakesheff, K. M.; Saunders, B.; Alexander, C., Biodegradable Thermoresponsive Microparticle Dispersions for Injectable Cell Delivery Prepared Using a Single-Step Process. Advanced Materials 2009, 21 (18), 1809-1813.

12. Qiao, M. X.; Chen, D. W.; Ma, X. C.; Liu, Y. J., Injectable biodegradable temperature-responsive PLGA-PEG-PLGA copolymers: Synthesis and effect of copolymer composition on the

drug release from the copolymer-based hydrogels. International Journal Of Pharmaceutics 2005, 294 (1-2), 103-112.

13. Fu, C.; Bai, H. T.; Zhu, J. Q.; Niu, Z. H.; Wang, Y.; Li, J. N.; Yang, X. Y.; Bai, Y. S., Enhanced cell proliferation and osteogenic differentiation in electrospun PLGA/hydroxyapatite nanofibre scaffolds incorporated with graphene oxide. Plos One 2017, 12 (11).

14. Panyam, J.; Labhasetwar, V., Dynamics of endocytosis and exocytosis of poly(D,L-lactide-co-glycolide) nanoparticles in vascular smooth muscle cells. Pharm Res 2003, 20 (2), 212-20.

15. Kakde, D.; Powell, L. G.; Bansal, K. K.; Howdle, S.; Irvine, D.; Mantovani, G.; Millar, G.; Dailey, L. A.; Stone, V.; Johnston, H. J.; Alexander, C., Synthesis, characterization and evaluation of in vitro toxicity in hepatocytes of linear polyesters with varied aromatic and aliphatic co-monomers. Journal of Controlled Release 2016, 244, 214-228.

16. Abdel-Mottaleb, M. M. A.; Beduneau, A.; Pellequer, Y.; Lamprecht, A., Stability of fluorescent labels in PLGA polymeric nanoparticles: Quantum dots versus organic dyes. International Journal of Pharmaceutics 2015, 494 (1), 471-478.

17. Chauhan, V. M.; Burnett, G. R.; Aylott, J. W., Dual-fluorophore ratiometric pH nanosensor with tuneable pK(a) and extended dynamic range. Analyst 2011, 136 (9), 1799-1801.

18. Horisawa, E.; Kubota, K.; Tuboi, I.; Sato, K.; Yamamoto, H.; Takeuchi, H.; Kawashima, Y., Size-dependency of DL-lactide/glycolide copolymer particulates for intra-articular delivery system on phagocytosis in rat synovium. Pharm Res 2002, 19 (2), 132-9.

19. Weiss, B.; Schaefer, U. F.; Zapp, J.; Lamprecht, A.; Stallmach, A.; Lehr, C. M., Nanoparticles made of fluorescence-labelled Poly(L-lactide-co-glycolide): preparation, stability, and biocompatibility. J Nanosci Nanotechnol 2006, 6 (9-10), 3048-56.

20. Ratzinger, G.; Fillafer, C.; Kerleta, V.; Wirth, M.; Gabor, F., The role of surface functionalization in the design of PLGA micro- and nanoparticles. Critical Reviews™ in Therapeutic Drug Carrier Systems 2010, 27 (1).

21. Conte, C.; Mastrotto, F.; Taresco, V.; Tchoryk, A.; Quaglia, F.; Stolnik, S.; Alexander, C., Enhanced uptake in 2D- and 3D- lung cancer cell models of redox responsive PEGylated nanoparticles with sensitivity to reducing extra- and intracellular environments. Journal of Controlled Release 2018, 277, 126-141.

22. Redhead, H. M.; Davis, S. S.; Illum, L., Drug delivery in poly(lactide-co-glycolide) nanoparticles surface modified with poloxamer 407 and poloxamine 908: in vitro characterisation and in vivo evaluation. Journal Of Controlled Release 2001, 70 (3), 353-363.

23. Chauhan, V. M.; Orsi, G.; Brown, A.; Pritchard, D. I.; Aylott, J. W., Mapping the Pharyngeal and Intestinal pH of Caenorhabditis elegans and Real-Time Luminal pH Oscillations Using Extended Dynamic Range pH-Sensitive Nanosensors. Acs Nano 2013, 7 (6), 5577-5587.

24. Harrison, R. P.; Chauhan, V. M.; Onion, D.; Aylott, J. W.; Sottile, V., Intracellular processing of silica-coated superparamagnetic iron nanoparticles in human mesenchymal stem cells. Rsc Advances 2019, 9 (6), 3176-3184.

25. Auwerx, J., The Human Leukemia-Cell Line, Thp-1 - A Multifaceted Model For The Study Of Monocyte-Macrophage Differentiation. Experientia 1991, 47 (1), 22-31.

26. Peng, Z.-H.; Kopeček, J., Enhancing Accumulation and Penetration of HPMA Copolymer–Doxorubicin Conjugates in 2D and 3D Prostate Cancer Cells via iRGD Conjugation with an MMP-2 Cleavable Spacer. Journal of the American Chemical Society 2015, 137 (21), 6726-6729.

27. Basuki, J. S.; Duong, H. T. T.; Macmillan, A.; Erlich, R. B.; Esser, L.; Akerfeldt, M. C.; Whan, R. M.; Kavallaris, M.; Boyer, C.; Davis, T. P., Using Fluorescence Lifetime Imaging Microscopy to Monitor Theranostic Nanoparticle Uptake and Intracellular Doxorubicin Release. Acs Nano 2013, 7 (11), 10175-10189.

28. Zhao, Y.-X.; Shaw, A.; Zeng, X.; Benson, E.; Nystrom, A. M.; Hogberg, B., DNA Origami Delivery System for Cancer Therapy with Tunable Release Properties. Acs Nano 2012, 6 (10), 8684–8691.

29. Wibroe, P. P.; Ahmadvand, D.; Oghabian, M. A.; Yaghmur, A.; Moghimi, S. M., An integrated assessment of morphology, size, and complement activation of the PEGylated liposomal doxorubicin products Doxil®, Caelyx®, DOXOrubicin, and SinaDoxosome. Journal of Controlled Release 2016, 221, 1-8.

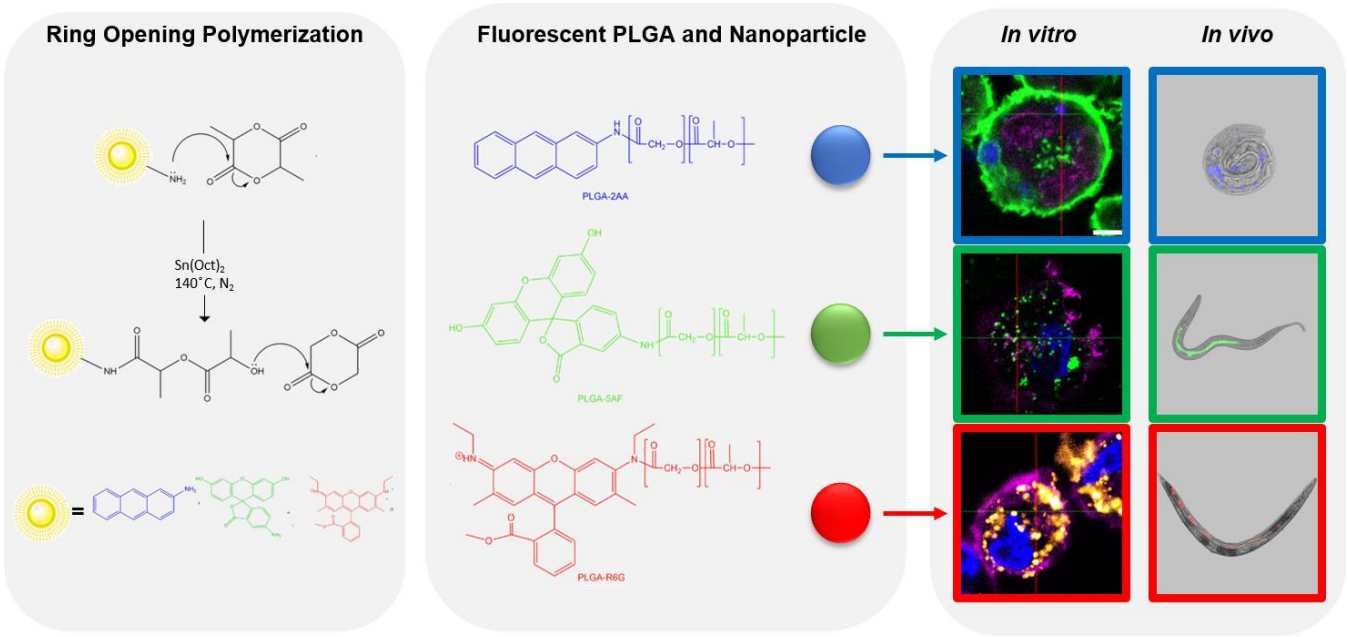

Fluorescent-dye initiated polymerisations of lactide and glycolide yield stable and bright fluorescent polymers in one step allowing facile sub-cellular tracking of drug delivery